Low-Latency MISO FBMC-OQAM: It Works for Millimeter Waves!

Ronald Nissel, Erich Zöchmann, Martin Lerch, Sebastian Caban, and Markus Rupp

Christian Doppler Laboratory for Dependable Wireless Connectivity for the Society in Motion,
Institute of Telecommunications, TU Wien, Vienna, 1040, Austria

***Abstract*—A key enabler for high data rates in future wireless systems will be the usage of millimeter Waves (mmWaves). Furthermore, Filter Bank Multi-Carrier (FBMC) with its good spectral properties has also been considered as a possible future transmission technique. However, many authors claim that multiple antennas and low-latency transmissions, two of the key requirements in 5G, cannot be efficiently supported by FBMC. This is not true in general, as we will show in this paper. We investigate FBMC transmissions over real world channels at 60 GHz and show that Alamouti's space time block code works perfectly fine once we spread (code) symbols in time. Although it is true that spreading increases the transmission time, the overall transmission time is still very low due to the high subcarrier spacing employed in mmWaves. Therefore, coded FBMC in combination with mmWaves enables high spectral efficiency, low-latency and allows the straightforward usage of multiple antennas.**

***Index Terms*—5G mobile communication, Millimeter wave measurements, Space-time codes, Code division multiplexing**

I. Introduction

Orthogonal Frequency Division Multiplexing (OFDM), currently employed in Long Term Evolution (LTE), applies a rectangular prototype filter, leading to high Out-Of-Band (OOB) emissions; not suitable for future wireless systems. There are methods to reduce the OOB emissions in OFDM, such as windowing or filtering, but they all have the disadvantage of reduced spectral efficiency. Filter Bank Multi-Carrier (FBMC) with Offset Quadrature Amplitude Modulation (OQAM), on the other hand, preserves high spectral efficiency at the expense of sacrificing the complex orthogonality condition with the less strict real orthogonality condition. This leads to additional challenges [1], especially for Multiple-Input Single-Output (MISO) [2] and channel estimation [3], [4]. Although it is true that many MISO methods cannot be directly employed in FBMC because the orthogonality condition is fulfilled in the real domain only, it is possible to recover complex orthogonality by precoding (spreading) symbols in time. This allows us to straightforwardly use all MISO methods known in OFDM. Such coding approach in the context of MISO was first proposed in [2] and later analyzed in more detail in [5]. The spreading process itself utilizes a fast Walsh-Hadamard transform so that the additional computational complexity is very low.

Besides new waveforms, millimeter Waves (mmWaves) will also be important in future wireless systems due to large available bandwidths in those frequency ranges [6]–[8]. Unfortunately, the propagation conditions of mmWaves are severely different compared to lower frequencies. Thus, extensive research is required to validate the applicability of mmWaves in practical systems. As proposed in [7] for mmWave transmissions, we also consider a high subcarrier spacing, inherently satisfying the low-latency condition.

The focus of this paper is the comparison of FBMC to OFDM in terms of Bit Error Ratio (BER). As we will show, FBMC and OFDM experience both the same BER and require approximately the same frame transmission time. Thus, utilizing OFDM, as currently done, for example, in IEEE 802.11ad, might not be optimal. Instead, FBMC might be a better solution because it offers a higher spectral efficiency.

Novel contribution: We present a 60 GHz measurement setup and show experimentally that, in contrast to common believe, low latency MISO works in FBMC.

II. System Model

The basic idea of multi-carrier systems is to transmit data symbols, usually chosen from a Quadrature Amplitude Modulation (QAM) signal constellation, over a rectangular time-frequency grid, so that the transmitted signal $s(t)$ can be written as [9]:

$$s(t) = \sum_{k=1}^{K} \sum_{l=1}^{L} g_{l,k}(t)\, x_{l,k}. \tag{1}$$

Here, $x_{l,k}$ denotes the transmitted symbol (at subcarrier-position l and time-position k) and $g_{l,k}(t)$ the corresponding basis pulse, essentially a time and frequency shifted prototype filter (we employ a Hermite prototype filter [10], [11]). The total number of subcarriers is given by L and the total number of time-symbols (per frame) by K.

Unfortunately, maximum spectral efficiency, time-localization, frequency-localization and orthogonality cannot be fulfilled at the same time according to the Balian-Low theorem [12]. In OFDM, the underlying rectangular function violates frequency localization, leading to high OOB emissions. Conventional FBMC-OQAM, on the other hand, replaces the complex orthogonality condition with the less strict real orthogonality condition, making the application of MISO more challenging. However, by spreading symbols in time (or frequency), we can restore complex orthogonality in FBMC-OQAM, so that MISO becomes as straightforward as in OFDM. For more information on such a coding approach we refer to our work in [5], which also includes a downloadable MATLAB code. Our measurements show that the channel is highly correlated in time and frequency. Thus, the channel induced inter-carrier interference and

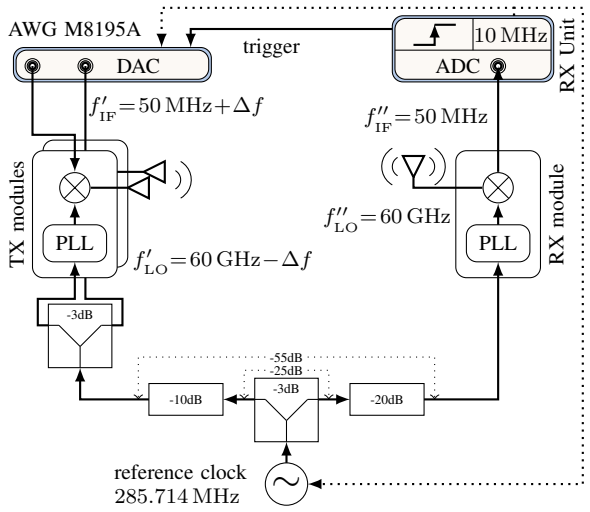

Fig. 1. Block diagram of our 60 GHz measurement setup. Fig. 2 shows pictures of our TX and RX modules. More information about our laboratory environment can be found in [13].

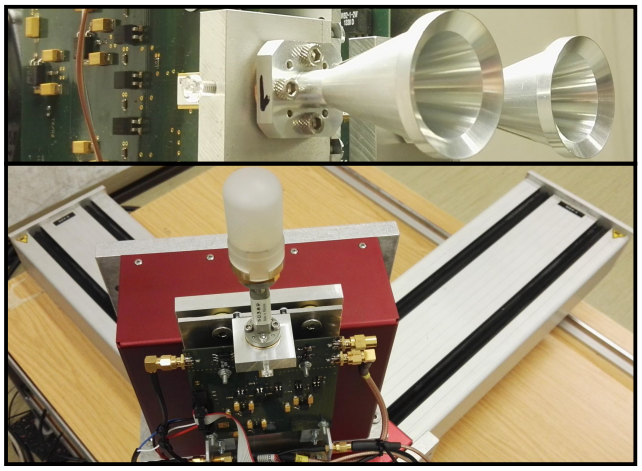

Fig. 2. Two 20 dBi conical horn TX antennas (top) and one omni-directional RX antenna (bottom) are located indoor, approximately 5 m apart. In order to obtain different channel realizations, we utilize an xy-table to relocate the RX antenna, resulting in Rician fading, see Fig. 3. In case of NLOS, we put an object between TX and RX, blocking most of the LOS components.

inter-symbol interference can be neglected. This allows us to accurately model the received symbols $y_{l,m}$ by:

$$y_{l,m} = h^{(1)}_{l,m} x^{(1)}_{l,m} + h^{(2)}_{l,m} x^{(2)}_{l,m} + n_{l,m}. \tag{2}$$

In OFDM, the subscript m describes the time index $m = k$ while in Coded-FBMC it describes the coding index. Furthermore, the superscript $(\cdot)^{(1)}$ indicates transmit antenna 1 and $(\cdot)^{(2)}$ transmit antenna 2. We consider Alamouti's space time block coding [2] as well as Single-Input Single-Output (SISO) transmissions, that is, $x^{(2)}_{l,m} = 0$. Our measurements show that the channel can be modeled by a Rician fading process, with $|h_{l,m}| \sim \mathrm{Rice}\left(\sqrt{\frac{\mathrm{K}}{\mathrm{K}+1}}, \frac{1}{\sqrt{2(\mathrm{K}+1)}}\right)$, where K is the Rician-K factor. The phase of $h_{l,m}$ is uniformly distributed and the channel between antenna 1 and antenna 2 is correlated, $\rho = \mathbb{E}\{|h^{(1)}_{l,m}||h^{(2)}_{l,m}|\}$. The variable $n_{l,m}$ describes the Gaussian distributed noise $n_{l,m} \sim \mathcal{CN}(0, P_{\mathrm{n}})$, with P_{n} denoting the noise power. The signal power, on the other hand, is defined as $P_{\mathrm{s}} = \mathbb{E}\{|h^{(1)}_{l,m} x^{(1)}_{l,m}|^2 + |h^{(2)}_{l,m} x^{(2)}_{l,m}|^2\}$. In order to validate our measurements, we compare them to simulations in case of Rician fading and to analytical expressions in case of an Additive White Gaussian Noise (AWGN) channel, $h_{l,m} = 1$.

III. mmWave Testbed

We use a similar methodology as for our measurements at 2.5 GHz [14]–[16]. FBMC and OFDM waveforms are generated off-line in MATLAB, digitally up-converted to an Intermediate Frequency (IF) and converted to the analog domain by an Arbitrary Waveform Generator (AWG) (8-bit, 16 GSamples/s). Our mmWave modules [17], [18] then up-convert this IF signal to 60 GHz, see Fig. 1. The receiver works in a similar way, but in reversed order. The received samples (16-bit, 200 MSamples/s) are also evaluated off-line in MATLAB. To guarantee time-synchronization, we employ a trigger network. The built-in synthesizer Phase-Locked Loop (PLL) is locking on a reference clock of 285.714 MHz and capable of synthesizing a frequency grid of $\Delta f = 285.714\,\mathrm{MHz} \cdot 7/4 \approx 500\,\mathrm{MHz}$ distance. To avoid IF crosstalk, we operate the transmitters and the receiver at different IFs. Furthermore, the mirror frequencies are suppressed as the Local Oscillator (LO) at the receiver is Δf higher than the LO at the transmitter.

A common reference clock is applied to all mmWave modules. To avoid any crosstalk on the common clock line, we increase the isolation by additional attenuators, see Fig. 1.

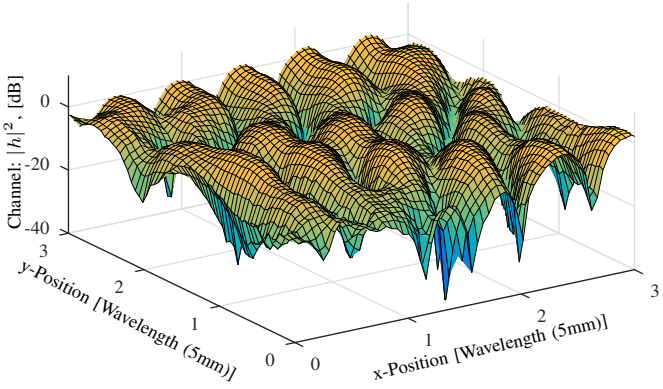

Fig. 3. The measured channel (averaged over 6 MHz and 300 μs, possible due to high correlation in time and frequency) shows large fading dips in case of NLOS (low Rician K factor). For LOS we observe smaller fluctuations due to a higher Rician K factor (not shown here).

IV. Measurement Results

Table I summarizes our measurement parameters. Note that in FBMC, pulses overlap in time (overlapping factor of 3), so that the transmission time in FBMC is 4 μs longer than in OFDM. However, the overall transmission time is still much lower than 100 μs, allowing low-latency transmissions [19]. For a fair comparison, OFDM and FBMC have the same transmit power $\mathbb{E}\{|s(t)|^2\}$, leading also to the same Signal-to-Noise Ratio (SNR) at the receiver. Furthermore, OFDM and

TABLE I
MEASUREMENT PARAMETERS

Carrier frequency	60 GHz
Subcarrier spacing, F	500 kHz
Number of subcarriers, L	48
Transmission bandwidth (without guard), FL	24 MHz
Number of (complex) time-symbols per frame, K	16
Frame transmission time for OFDM (with cyclic prefix)	33 μs
Frame transmission time for FBMC (with guard+overlap)	33 μs + 4 μs
Signal constellation	4-QAM
Bit rate (ignoring pilots)	46.5 MBit/s
Pilot spacing in frequency (diamond shaped)	6
Pilot spacing in time (diamond shaped)	8
Number of random RX positions (xy-table)	1000
RX positioning area in wavelengths (5mm)	7×6

TABLE II
MEASURED CHANNEL PARAMETERS

	Rician K Ant. 1	Rician K Ant. 2	Ant. correlation, ρ
LOS	24	42	0.2
NLOS	0.9	2.9	0.4

FBMC have the same bit rate, but FBMC has better spectral properties and therefore a higher spectral efficiency.

The interference plus noise power is estimated by evaluating the received symbols at subcarrier position 0 and $L+1$, that is, the first subcarrier below and above the transmission band. On the other hand, the noise power is estimated by setting all transmitted symbols to zero, $x_{l,m}^{(1)} = x_{l,m}^{(2)} = 0$. Our setup behaves linearly within the considered transmit power range. However, phase noise causes severe self interference, leading to a Signal-to-Interference Ratio (SIR) of approximately 17 dB.

We measure three different scenarios: Line-Of-Sight (LOS), Non-Line-Of-Sight (NLOS) and AWGN. For the NLOS case, we block the direct path by an object. This causes a loss in received signal power by approximately 10 dB that we compensate by increasing the transmit power. For the AWGN scenario (SISO), we connect the TX module and the RX module back-to-back with 60 dB attenuation.

Our measurements show that the channel is highly correlated in time and frequency. Indeed, the correlation coefficient in time is approximately one for all scenarios. The correlation coefficient in frequency is also approximately one, except for antenna 1 in case of NLOS, where we observe a correlation coefficient between the first and the last subcarrier (23.5 MHz) of 0.83.

As shown in Table I, our transmission bandwidth of $FL = 24$ MHz is relatively narrow (for mmWaves). This is due to the sampling rate of our analog-to-digital converter (a maximum of 100 MHz would be possible, but filters and robustness to crosstalk prevents us from doing that). Furthermore, a narrow bandwidth guarantees a sufficiently high SNR at the receiver (we currently do not employ a power amplifier). However, the bandwidth has no impact on the (averaged) uncoded BER.

Our measurement results also include a confidence interval obtained by bootstrapping [20]. For each RX position, we average the BER over one transmission block. On these measurement results we then apply the MATLAB built-in bootstrap function.

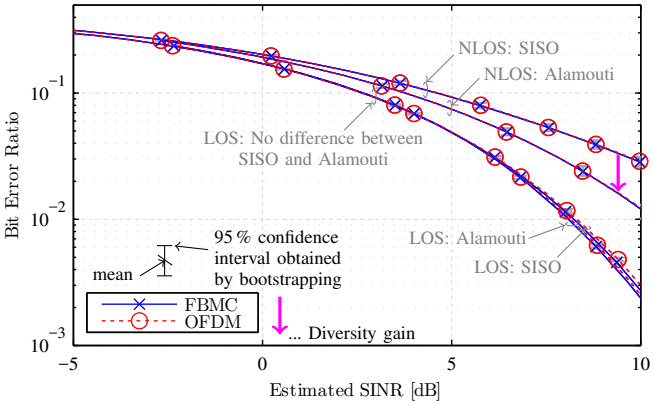

Fig. 4. FBMC performs as good as OFDM in terms of BER, but has the additional advantage of much lower out-of-band emissions. Alamouti's space time block code improves the performance in case of NLOS but not for LOS because there is almost no diversity to exploit.

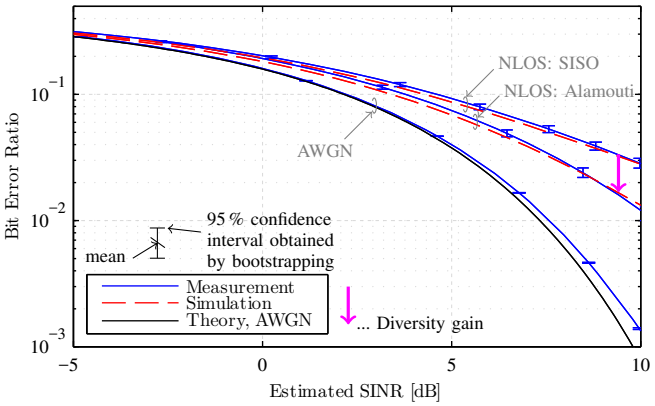

Fig. 5. The system model in (2) accurately describes our measurement results. The simulation parameters can be found in Table II while for AWGN we rely on theoretical expressions (complementary error function). In case of AWGN, the small deviation between theory and measurements can be explained by hardware effects.

Fig. 4 compares OFDM and FBMC in terms of BER over estimated Signal-to-Interference plus Noise Ratio (SINR) for the LOS and the NLOS scenario. In FBMC we observe the same BER as in OFDM, but FBMC has better spectral properties [5]. Thus, if high spectral efficiency is the primary goal, FBMC should be chosen over OFDM (which, however, has a slightly lower computational complexity). We further see that Alamouti's space time block code provides no diversity gain in case of LOS. Once the direct path is blocked, however, Alamouti's space time block code exploits spatial diversity, increasing the overall robustness of the system. Note that the BER is relatively high due to the random fading dips, see Fig. 3. In practice, we would include channel coding.

Fig. 5 shows the measurement results for FBMC and compares them to our system model in (2). Overall, we see a good match between theory and measurements. In case of AWGN, we observe small deviations starting at approximately 5 dB which can be explained by non-Gaussian interference.

V. Conclusion

Spreading symbols in time allows us to restore complex orthogonality in FBMC-OQAM, so that all MISO methods known in OFDM can be straightforwardly applied. We showed through real world testbed measurements that for such coding scheme, FBMC has the same BER as OFDM but the additional advantage of lower OOB emissions. Furthermore, the high subcarrier spacing proposed for mmWaves [7] leads to a reduced transmission time, allowing low latency communications despite the increased frame duration due to spreading. Thus, the requirements of 5G can be perfectly met by Coded-FBMC in mmWave communications.

In case of LOS, Alamouti's space time block code shows no improvement compared to SISO. However, once the direct path is blocked, such spatial diversity scheme improves the performance. This is particularly useful in mmWave communications where the LOS path might easily be blocked.

Acknowledgment

The financial support by the Austrian Federal Ministry of Science, Research and Economy, the National Foundation for Research, Technology and Development, and the TU Wien is gratefully acknowledged.

References

[1] A. A. Zaidi, J. Luo, R. Gerzaguet, A. Wolfgang, R. J. Weiler, J. Vihriala, T. Svensson, Y. Qi, H. Halbauer, Z. Zhao *et al.*, "A preliminary study on waveform candidates for 5G mobile radio communications above 6 GHz," in *IEEE Vehicular Technology Conference (VTC Spring)*, 2016.

[2] C. Lélé, P. Siohan, and R. Legouable, "The Alamouti scheme with CDMA-OFDM/OQAM," *EURASIP Journal on Advances in Signal Processing*, 2010.

[3] R. Nissel and M. Rupp, "Bit error probability for pilot-symbol aided channel estimation in FBMC-OQAM," in *IEEE International Conference on Communications (ICC)*, 2016.

[4] R. Nissel, E. Zöchmann, and M. Rupp, "On the influence of doubly-selectivity in pilot-aided channel estimation for FBMC-OQAM," in *IEEE Vehicular Technology Conference (VTC Spring)*, 2017.

[5] R. Nissel and M. Rupp, "Enabling low-complexity MIMO in FBMC-OQAM," in *IEEE Globecom Workshops (GC Wkshps)*, 2016.

[6] T. S. Rappaport, S. Sun, R. Mayzus, H. Zhao, Y. Azar, K. Wang, G. N. Wong, J. K. Schulz, M. Samimi, and F. Gutierrez, "Millimeter wave mobile communications for 5G cellular: It will work!" *IEEE Access*, vol. 1, pp. 335–349, 2013.

[7] Z. Pi and F. Khan, "An introduction to millimeter-wave mobile broadband systems," *IEEE Communications Magazine*, vol. 49, no. 6, pp. 101–107, June 2011.

[8] E. Zöchmann, S. Schwarz, and M. Rupp, "Comparing antenna selection and hybrid precoding for millimeter wave wireless communications," in *IEEE Sensor Array and Multichannel Signal Processing Workshop (SAM)*, 2016.

[9] R. Nissel and M. Rupp, "OFDM and FBMC-OQAM in doubly-selective channels: Calculating the bit error probability," *IEEE Communications Letters*, 2017, accepted for publication.

[10] R. Haas and J.-C. Belfiore, "A time-frequency well-localized pulse for multiple carrier transmission," *Wireless Personal Communications*, vol. 5, no. 1, pp. 1–18, 1997.

[11] R. Nissel and M. Rupp, "On pilot-symbol aided channel estimation in FBMC-OQAM," in *IEEE International Conference on Acoustics, Speech and Signal Processing (ICASSP)*, 2016.

[12] H. G. Feichtinger and T. Strohmer, *Gabor analysis and algorithms: Theory and applications*. Springer Science & Business Media, 2012.

[13] E. Zöchmann, M. Lerch, S. Caban, R. Langwieser, C. Mecklenbräuker, and M. Rupp, "Directional evaluation of receive power, Rician K-factor and RMS delay spread obtained from power measurements of 60 GHz indoor channels," in *IEEE Topical Conference on Antennas and Propagation in Wireless Communications (APWC)*, 2016.

[14] R. Nissel, S. Caban, and M. Rupp, "Experimental evaluation of FBMC-OQAM channel estimation based on multiple auxiliary symbols," in *IEEE Sensor Array and Multichannel Signal Processing Workshop (SAM)*, 2016.

[15] S. Caban, J. A. García-Naya, and M. Rupp, "Measuring the physical layer performance of wireless communication systems," *IEEE Instrumentation & Measurement Magazine*, vol. 14, no. 5, pp. 8–17, 2011.

[16] R. Nissel, S. Caban, and M. Rupp, "Closed-Form capacity expression for low complexity BICM with uniform inputs," in *IEEE International Symposium on Personal, Indoor and Mobile Radio Communications (PIMRC)*, 2015.

[17] P. Zetterberg and R. Fardi, "Open source SDR frontend and measurements for 60-GHz wireless experimentation," *IEEE Access*, vol. 3, pp. 445–456, 2015.

[18] Pasternack: 60 GHz transmitter and 60 GHz receiver modules. [Online]. Available: https://www.pasternack.com/60-ghz-modules-category.aspx

[19] G. P. Fettweis, "The tactile internet: Applications and challenges," *IEEE Vehicular Technology Magazine*, vol. 9, no. 1, pp. 64–70, 2014.

[20] B. Efron and R. J. Tibshirani, *An introduction to the bootstrap*. CRC press, 1994.